AIP | Applied Physics Letters

High efficiency rare-earth emitter for thermophotovoltaic applications

E. S. Sakr, Z. Zhou, and P. Bermel

Citation: Applied Physics Letters **105**, 111107 (2014); doi: 10.1063/1.4895932
View online: http://dx.doi.org/10.1063/1.4895932
View Table of Contents: http://scitation.aip.org/content/aip/journal/apl/105/11?ver=pdfcov
Published by the AIP Publishing

High efficiency rare-earth emitter for thermophotovoltaic applications

E. S. Sakr, Z. Zhou, and P. Bermel[a)]
Birck Nanotechnology Center, School of Electrical and Computer Engineering, Purdue University, 1205 W. State St., West Lafayette, Indiana 47907, USA

(Received 30 July 2014; accepted 4 September 2014; published online 16 September 2014)

In this work, we propose a rare-earth-based ceramic thermal emitter design that can boost thermophotovoltaic (TPV) efficiencies significantly without cold-side filters at a temperature of 1573 K (1300 °C). The proposed emitter enhances a naturally occurring rare earth transition using quality-factor matching, with a quarter-wave stack as a highly reflective back mirror, while suppressing parasitic losses via exponential chirping of a multilayer reflector transmitting only at short wavelengths. This allows the emissivity to approach the blackbody limit for wavelengths overlapping with the absorption peak of the rare-earth material, while effectively reducing the losses associated with undesirable long-wavelength emission. We obtain TPV efficiencies of 34% using this layered design, which only requires modest index contrast, making it particularly amenable to fabrication via a wide variety of techniques, including sputtering, spin-coating, and plasma-enhanced chemical vapor deposition. © *2014 AIP Publishing LLC*. [http://dx.doi.org/10.1063/1.4895932]

Thermophotovoltaic (TPV) systems convert thermal energy directly into electricity.[1] Sufficiently, energetic thermal photons are converted into electricity by a photovoltaic (PV) cell. A typical TPV system consists of a high-temperature emitter, a filter, and a PV cell.[2] The heat source can be a gas burner,[3] concentrated solar power,[4] or a catalytic microcombustor.[5] Most of the losses in the TPV system are caused by sub-bandgap emitted photons, which cannot be absorbed by the PV cell to produce electron-hole pairs.[6] Consequently, spectral shaping to suppress sub-bandgap photon emission and enhance photon emission with energies larger than the bandgap of the PV cell is required.[2,6] These two requirements can be achieved by using selective emitters and filters.[1] One possible approach to design such a selective emitter is the use of 1D, 2D, and 3D photonic crystals.[6–9] Another approach is based on rare-earth emitters that naturally display selective emission at certain wavelengths,[2] which can be matched to available PV cell technologies.

An example of a selective thermal emitter based on rare-earth oxides was investigated in Bitnar's work.[2] Another example based on rare-earth ceramic selective emitters was investigated in Chubb's work,[10,11] in which the Erbium-doped Aluminum Garnet (ErAG), was shown to have the largest extinction coefficient at 1.47 μm and 1.53 μm; hence, by Kirchoff's law of thermal radiation,[12] an optically thick ErAG film on a platinum substrate produced selective spectral emittance around 1.5 μm at a substrate temperature of 1635 K. However, the radiative efficiency alone was as low as 20% at a substrate temperature of 1635 K,[10] and a significant parasitic long-wavelength emission tail was present, despite the very low extinction coefficient of the ErAG in the range from 2 μm to 5 μm. This is mainly caused by the use of a thick ErAG film to achieve high emittance at shorter wavelengths, as well as Ohmic losses from the platinum substrate.

In this work, a much higher efficiency ErAG emitter structure is introduced, which both enhances emission for energies above the bandgap and suppresses emission below the bandgap. It is also top-surface emitting, so that emission is directed almost exclusively towards a single set of PV cells above. To achieve this performance, we use a high-temperature dielectric mirror[13] as a substrate and a partially transmissive dielectric mirror on top of the ErAG film. Following previous work,[7] the loss rate in the ErAG is matched to the loss rate of the partially transmissive dielectric mirror on top of the structure; this process is referred to as quality-factor matching (Q-matching),[14,15] and yields near-blackbody emissivity. Furthermore, an exponentially chirped multi-layer dielectric filter can be placed on top of the film to suppress a significant part of the sub-bandgap emission, while transmitting above-bandgap photons. The proposed ErAG emitter is suitable for operation with GaSb PV cells. Assuming reasonable PV cell performance, the theoretical TPV efficiency is shown to reach 34%. Such a multi-layer structure can be fabricated using different deposition techniques. Comparable examples of fabricated silicon dioxide (SiO_2)/titanium dioxide (TiO_2) multi-layers using reactive magnetron sputtering,[16–19] sol-gel methods combined with spin-coating,[20–22] and Plasma-Enhanced Chemical Vapor Deposition (PECVD)[23] have been demonstrated in recent work.

In this paper, we will first explain the details of our methodology for calculating selective emitter spectra and the resulting TPV system efficiency. Second, we will discuss various approaches to improve the efficiency of the ErAG emitter, including the high efficiency ErAG emitter design proposed in this paper, with the results for the spectral emittance and TPV efficiency. Then a discussion of the significance of these results is provided, which ends with the key conclusions.

To simulate multi-layered structures for our selective emitters, we use the Stanford Stratified Structure Solver (S4),[24] a frequency domain code that solves Maxwell's equations in layered periodic structures using coupled wave

[a)]Author to whom correspondence should be addressed. Electronic mail: pbermel@purdue.edu.

analysis and scattering matrix algorithm.[25] According to Kirchhoff's law of thermal radiation, for a body emitting and absorbing thermal radiation in thermodynamic equilibrium, the emissivity is equal to the absorptivity for every wavelength.[12] Hence, the key goal of the emitter design is to spectrally shape the absorption, according to the requirements of the target emittance design. Using S4, a normally incident plane wave is excited in the semi-infinite vacuum top layer of the structure, the reflectance (R) and transmittance (T) are computed; hence, the emittance is simply the absorption $A = 1-R-T$.

Once the emittance spectrum is obtained, the efficiency of the TPV system can be estimated. The TPV efficiency is given by $\eta = J_{SC}V_{OC}FF/P_{emit}$, where J_{SC} is the short circuit current density, V_{OC} is the open-circuit voltage, FF is the fill factor, and P_{emit} is the blackbody integrated emitted thermal power density. The current density in the PV cell is a contribution of two components: the photo-current density induced in the PV cell by the incident thermal photons and the dark current density that flows in the PV cell in the absence of incident radiation. Hence, the total current density is given by

$$J = \int_0^\infty d\lambda \left[\frac{2qc}{\lambda^4}\frac{\varepsilon(\lambda)\mathrm{EQE}(\lambda)}{\exp(hc/\lambda kT_e)-1}\right] - J_0 \exp\left(-\frac{E_g}{kT_d}\right) \times \left[\exp\left(\frac{qV}{mkT_d}\right) - 1\right], \quad (1)$$

where q is the electron charge, c is the speed of light in vacuum, λ is the wavelength, $\varepsilon(\lambda)$ is the spectral emittance of the emitter, $\mathrm{EQE}(\lambda)$ is the external quantum efficiency of the device, h is Planck's constant, k is Boltzmann's constant, E_g is the PV cell bandgap in eV, $J_o = 5693E_g^2$ A/cm^2 is the thermodynamically required dark current density prefactor,[26] V is the voltage, T_d is the device temperature, and m is the device ideality factor. From Eq. (1), J_{SC} and V_{OC} can be computed; hence, the fill factor is estimated from well-known empirical relations.[27] All the TPV efficiency computations are implemented in a nanoHUB tool named TPV efficiency simulation.[28] The emittance results obtained from S4 are fed to the TPV efficiency simulation tool to calculate the TPV efficiency under different operating conditions. The PV diode is assumed to have bandgap energy of 0.75 eV, which resembles an arsenide-doped GaSb PV cell. The device ideality factor and the EQE of the PV cell values are taken from previous experimental work.[5] All the TPV efficiencies estimated here assume a matching rugate filter in the TPV system, unless otherwise is stated.

As shown in previous work, the metallic ErAG emitter has shown promise but limited overall spectral efficiency. As a first step, one would like to eliminate the Ohmic losses of the platinum substrate, by using the ErAG itself as a low-loss substrate. We first consider two different ErAG emitter designs based on this concept: an ErAG film with anti-reflection (AR) coatings on both sides of the film, and the high efficiency ErAG emitter using dielectric mirrors.

In order to eliminate the losses associated with the metallic substrate, it can be replaced by an AR coating on the bottom of the ErAG film, but this configuration allows both top and bottom emission. So, another AR coating can be applied on the top of the ErAG film, so that a symmetrically emitting configuration is obtained, allowing for the use of two sets of PV cells, on top and bottom sides of the emitter. The two AR coatings prevent multiple reflections at the ErAG film edges, allowing maximum absorption within the film at 1.47 μm.

The emittances at two different film thicknesses are shown in Fig. 1. As expected, the thicker the film is, the larger the emission is all over the spectrum. Because of the increased parasitic emission of sub-bandgap photons, the TPV efficiency degrades as the film thickness increases from 125 μm to 250 μm, as shown in Table I.

The latter configuration lacks the asymmetric emission property, and still suffers high parasitic sub-bandgap losses, due to the thick ErAG film losses. Hence, to keep the asymmetric emission property while eliminating the metallic substrate absorption losses, the reflecting metal substrate used in Ref. 10 is replaced by a highly reflective quarter-wave stack dielectric mirror, with the lowest frequency band of full-reflection centered at 1.5 μm. Moreover, the concept of Q-matching[14,15] can be used to enhance the emission above the bandgap. Following the same procedure in Ref. 7, at normal incidence, absorption losses in the ceramic film can be matched to the transmissive losses through the top mirror at a resonant wavelength of 1.47 μm. Because the absorption loss rate is small at this wavelength, the resulting resonant mode will not be suitable for TPV conversion.[6] Hence, the ErAG film thickness should be increased to form a multi-mode Fabry-Perot resonant cavity with very narrow spaces between modes.

A further improvement to suppress the parasitic emission is to use an exponentially chirped filter on top of the structure, such that a wide band of long wavelength emission can be significantly eliminated. The chirped mirror will have a strong reflection band from 2 μm to 4 μm, so that the emissive blackbody power in this range at emitter temperature of 1573 K will be significantly minimized. This configuration has the advantage of having the filter integrated with the emitter, so that expensive filters, such as rugate filters,[29] can

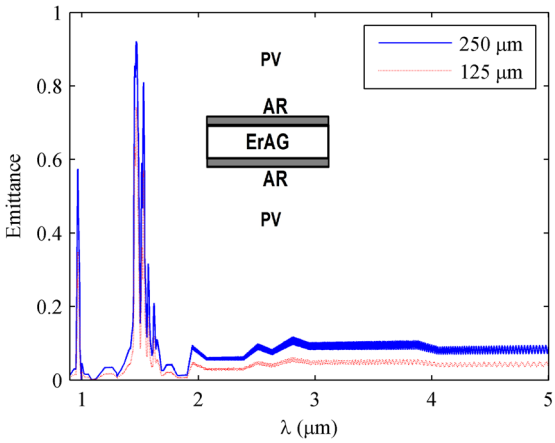

FIG. 1. Emittance spectrum of an ErAG emitter with AR coatings at different thicknesses. Although short-wavelength emission increases with thickness, so do parasitic losses at longer wavelengths, limiting overall spectral efficiencies.

TABLE I. TPV efficiency for different ErAG emitter designs. Although all designs display overall efficiencies higher than seen for metal substrates, the best overall performance comes from the chirped filter + shifted rugate filter at 33.89%.

ErAG emitter	d (μm)	η (%) at 1323 K	η (%) at 1573 K	η_{rad} (%) at 1573 K	$\bar{\varepsilon}$ (%) at 1573 K	Top/bottom layers
AR + rugate filter	125	12.6	19.18	41.4	5.09	1/1
AR + rugate filter	250	12.05	18.63	37	9.26	1/1
Q-matched + rugate filter	125	17	24.32	51.4	6.12	3/21
Q-matched + rugate filter	250	15.34	22.58	44.53	10.44	3/21
Chirped filter + shifted rugate filter	250	25.55	33.89	70.85	6.11	Chirped 26/21
Chirped filter only	250	25.46	32.94	70.85	6.11	Chirped 26/21

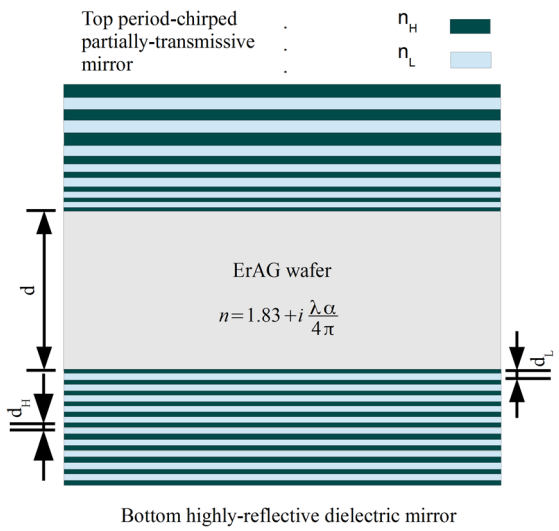

FIG. 2. A schematic of the high efficiency ErAG emitter with chirped-mirror. The bottom dielectric mirror is a quarter-wave stack with reflection centered at 1.47 μm. The low-index material thickness is $d_L = \lambda/4n_L$, and the high-index material thickness is $d_H = \lambda/4n_H$. The top dielectric mirror has an exponentially chirped period with up to 26 layers that reflects all the wavelengths from 2 μm to 4 μm. The ErAG wafer is assumed to be much thicker than the dielectric layers surrounding it.

be removed from the TPV system. The proposed ErAG emitter with chirped mirror is shown in Fig. 2.

The resulting emittance spectra for the loss-matched design without a chirped filter are shown in Fig. 3, where two different film thicknesses are simulated, and the dielectric mirrors are assumed to be a quarter-wave stack with $n_H = 2$ and $n_L = 1.414$, where n_H and n_L are the refractive indices of the high- and low-index materials, respectively. Values of the corresponding TPV efficiencies are shown in Table I. It is notable that increasing the thickness degrades the efficiency because sub-bandgap losses increase while the Q-matching guarantees an almost 100% emittance around 1.47 μm as shown in Fig. 3. However, this improves the TPV efficiency substantially to 24%, if compared to the corresponding efficiency in the AR coatings configuration.

If the partially transmissive mirror is replaced by an exponentially chirped period filter, a wide band of low frequencies beyond the bandgap will be reflected, as shown in Fig. 4, and this in turn will lead to a pronounced increase in the TPV efficiency. As shown in Table I, the TPV efficiency can reach almost 34% if the chirped filter emitter is used with a cold-side rugate filter with shifted cut-off to minimize losses beyond 3.5 μm. The TPV efficiency also reaches 33% if the chirped filter emitter design is used without any external filters. To measure the selectivity of the emitter, the radiation spectral efficiency η_{rad} is computed as in previous work.[10] It is obvious that the chirped filter increases the radiation efficiency, which translates into an improved TPV efficiency, as shown in Table I.

The high-efficiency ErAG emitter is a simple multilayer structure that can be fabricated without the need for sub-micron lithography fabrication techniques used for many optical 2D and 3D photonic crystal emitters. This design can be fabricated by depositing the dielectric quarter-wave layers

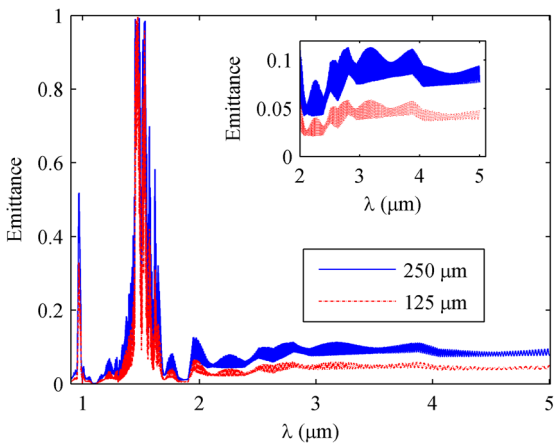

FIG. 3. Emittance spectrum of an ErAG film with a fully reflective back dielectric mirror and a loss-matched top dielectric mirror at different ErAG film thicknesses. The resulted curve is not smoothed to show Q-matched Fabry-Perot modes.

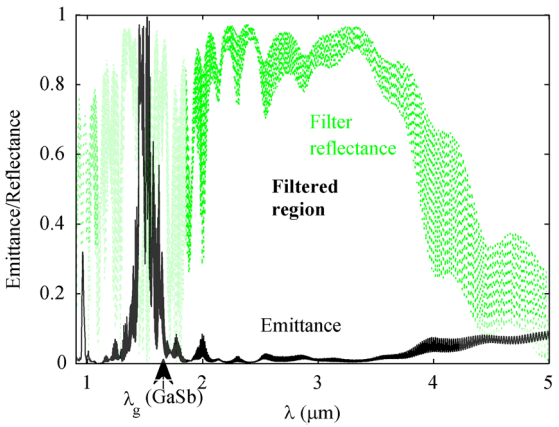

FIG. 4. Emittance spectrum of the highest efficiency ErAG emitter shown in Fig. 2. The ErAG film thickness is 250 μm. The exponentially chirped dielectric mirror filter on the top eliminates a wide band of parasitic emission beyond the bandgap wavelength. The resulted curve is not smoothed to show Q-matched Fabry-Perot modes.

on one side of an ErAG substrate, then depositing the chirped dielectric layers on the other side of the substrate. Key concerns for experimental fabrication, which can be mitigated through proper design choice, include the mechanical stability of the ErAG substrate and the robustness of the multi-layer structure at high temperatures. The ErAG substrate should be sufficiently thick to avoid the fracture of the substrate; hence, a 250 μm thick slab is the minimum recommended practical choice. Also, the dielectric materials involved in the dielectric mirror design should have a sufficiently high melting point and matching thermal expansion coefficients at high temperatures. Eligible material systems are SiO_2 and Tantalum oxide (Ta_2O_5), or SiO_2 and TiO_2. Obviously, if the refractive index contrast of the two materials is greater, fewer layers are needed, which makes the SiO_2/TiO_2 system simpler to fabricate than the SiO_2/Ta_2O_5 system. An additional strategy that can be useful is to alternate tensile and compressive stresses in each layer of the structure, to achieve zero residual stress for the overall multilayer stack.[30]

For practical TPV systems, other heat losses should be considered, such as losses due to heat conduction and convection.[1] Hence, the emitted power should be sufficiently high to minimize the impact of those losses. For this purpose, the average emissivity ($\bar{\varepsilon}$),[5] which gives the ratio of the emitted power to the total blackbody power at the emitter temperature, of each of the previous designs is computed. The average emissivity, as listed in Table I, decreases in the presence of the chirped filter, because a portion of the input power is reflected by the chirped mirror back to the source. However, this loss is compensated by the high TPV efficiency.

In this work, rare-earth doped ceramic thermal emitters were renovated to substantially enhance the TPV system efficiency. The proposed thermal emitter was shown to have theoretical TPV efficiency as high as 33% in absence of external filters. Its integrated filtering property can be achieved using a chirped dielectric mirror, which is easy to fabricate. Replacing the metallic substrate in previous designs by a dielectric mirror guarantees asymmetric radiation without any metallic losses. This thermal emitter can be optimized to provide enhanced selective radiation and low parasitic losses that can be matched to available GaSb PV cell technology, or other materials like germanium with similar bandgaps. Furthermore, the design idea can be generalized to a broad range of emitter materials demonstrating highly selective absorption, given an appropriate PV diode material.

We thank Qingshuang Chen and Anubha Mathur for providing access to simulation capabilities for this study. Support was provided by the Department of Energy, under DOE Cooperative Agreement No. DEEE0004946 (PVMI Bay Area PV Consortium), as well as the Semiconductor Research Corporation, under Research Task No. 2110.006 (Network for Photovoltaic Technologies). Computational resources on nanoHUB.org were provided by the Network for Computational Nanotechnology, which is funded by the U.S. National Science Foundation under Grant No. EEC-1227110.

[1]T. Bauer, *Thermophotovoltaics: Basic Principles and Critical Aspects of System Design* (Springer, Berlin, 2011).
[2]B. Bitnar, W. Durisch, and R. Holzner, Appl. Energy **105**, 430 (2013).
[3]B. Bitnar, W. Durisch, J.-C. Mayor, H. Sigg, and H. R. Tschudi, Sol. Energy Mater. Sol. Cells **73**, 221 (2002).
[4]V. Rinnerbauer, A. Lenert, D. M. Bierman, Y. X. Yeng, W. R. Chan, R. D. Geil, J. J. Senkevich, J. D. Joannopoulos, E. N. Wang, M. Soljačić, and I. Celanovic, Adv. Energy Mater. **4**, 1400334 (2014)
[5]P. Bermel, M. Ghebrebrhan, W. Chan, Y. X. Yeng, M. Araghchini, R. Hamam, C. H. Marton, K. F. Jensen, M. Soljačić, J. D. Joannopoulos, S. G. Johnson, and I. Celanovic, Opt. Express **18**, A314 (2010).
[6]E. Rephaeli and S. Fan, Opt. Express **17**, 15145 (2009).
[7]I. Celanovic, D. Perreault, and J. Kassakian, Phys. Rev. B **72**, 075127 (2005).
[8]I. Celanovic, N. Jovanovic, and J. Kassakian, Appl. Phys. Lett. **92**, 193101 (2008).
[9]M. De Zoysa, T. Asano, K. Mochizuki, A. Oskooi, T. Inoue, and S. Noda, Nat. Photonics **6**, 535 (2012).
[10]D. Chubb, A. Pal, M. Patton, and P. Jenkins, J. Eur. Ceram. Soc. **19**, 2551 (1999).
[11]B. S. Good, D. A. Chubb, and A. Pal, in *Fourth NREL Conference on Thermophotovoltaic Generation of Electricity* (AIP Publishing, Denver, Colorado (USA), 1999), pp. 214–223.
[12]G. B. Rybicki and A. P. Lightman, *Radiative Processes in Astrophysics* (Wiley-VCH Verlag GmbH, Weinheim, Germany, 1985).
[13]J. H. Apfel, Appl. Opt. **21**, 733 (1982).
[14]H. Haus, *Waves and Fields in Optoelectronics* (Prentice Hall, Inc., Englewood Cliffs, NJ, 1984), pp. 197–205.
[15]J. D. Joannopoulos, S. G. Johnson, J. N. Winn, and R. D. Meade, *Photonic Crystals Molding the Flow of Light*, 2nd ed. (Princeton University Press, Princeton, NJ, 2008).
[16]K. Wasa and S. Hayakawa, *Handbook of Sputter Deposition Technology: Principles, Technology, and Applications* (Noyes Publications, Park Ridge, NJ, 1992).
[17]O. Deparis, M. Rassart, C. Vandenbem, V. Welch, J.-P. Vigneron, L. Dreesen, and S. Lucas, Plasma Processes Polym. **6**, S746 (2009).
[18]S. Chao, W. H. Wang, and C. C. Lee, Appl. Opt. **40**, 2177 (2001).
[19]M. Mazur, D. Wojcieszak, J. Domaradzki, D. Kaczmarek, and S. Song, Opto-Electron. Rev. **21**, 233 (2013).
[20]S. Colodrero, M. Ocaña, and H. Míguez, Langmuir **24**, 4430 (2008).
[21]O. Sánchez-Sobrado, M. E. Calvo, N. Núñez, M. Ocaña, G. Lozano, and H. Míguez, Nanoscale **2**, 936 (2010).
[22]O. Sańchez-Sobrado, A. M. Yacomotti, M. E. Calvo, O. E. Martínez, M. Ocaña, N. Núñez, J. A. Levenson, and H. Míguez, Appl. Phys. Lett. **99**, 051111 (2011).
[23]J. Kowalski, H. Szymanowski, A. Sobczyk-Guzenda, and M. Gazicki-Lipman, Bull. Polish Acad. Sci. Tech. Sci. **57**, 171 (2009).
[24]J. Kang, X. Wang, P. Bermel, and C. Liu, "S4: Stanford Stratified Structure Solver" (2013), https://nanohub.org/resources/s4sim.
[25]V. Liu and S. Fan, Comput. Phys. Commun. **183**, 2233 (2012).
[26]C. H. Henry, J. Appl. Phys. **51**, 4494 (1980).
[27]M. A. Green, Solid-State Electron. **24**, 788 (1981).
[28]Q. Chen, P. Bermel, R. Shugayev, M. Sumino, Z. Zho, and R. Y. Omar, "TPV Efficiency Simulation" (2013), https://nanohub.org/resources/tpvtest.
[29]U. Ortabasi, in *Fifth Conference on Thermophotovoltaic Generation of Electricity* (AIP Publishing, Rome, Italy, 2003), pp. 249–258.
[30]J. Yang, H. Kahn, and A. He, J. Microelectromech. Syst. **9**, 485 (2000).